

Raman spectroscopic characterization of crater walls formed upon single-shot high energy femtosecond laser irradiation of dimethacrylate polymer doped with plasmonic gold nanorods

István Rigó¹, Judit Kámán¹, Ágnes Nagyné Szokol¹, Attila Bonyár², Melinda Szalóki³, Alexandra Borók^{1,2}, Shereen Zangana², Péter Rácz¹, Márk Aladi¹, Miklós Ákos Kedves¹, Gábor Galbács⁵, László P. Csernai^{1,6,7}, Tamás S. Biró¹, Norbert Kroó^{1,8}, Miklós Veres¹, NAPLIFE Collaboration

¹Wigner Research Centre for Physics, Budapest, Hungary

²Department of Electronics Technology, Faculty of Electrical Engineering and Informatics, Budapest University for Economics and Informatics, Budapest, H1111, Hungary

³Department of Biomaterials and Prosthetic Dentistry, Faculty of Dentistry, University of Debrecen, Debrecen, Hungary

⁴Centre for Energy Research, Institute of Technical Physics and Materials Science (MFA), H1121 Budapest, Hungary

⁵Department of Inorganic and Analytical Chemistry, University of Szeged, Szeged, H-6720 Hungary

⁶Department of Physics and Technology, University of Bergen, 5007 Bergen, Norway

⁷Frankfurt Institute for Advanced Studies, Frankfurt/Main, Germany

⁸Hungarian Academy of Sciences, 1051 Budapest, Hungary

Abstract

The changes in the bonding configuration on the crater walls formed in urethane dimethacrylate based polymer doped with plasmonic gold nanorods upon irradiation with a single-shot high energy femtosecond laser pulse has been studied by Raman spectroscopy. New Raman bands were detected in the 2000-2500 cm⁻¹ region of the Raman spectrum the intensities of which show strong dependence on the concentration of plasmonic nanoparticles and the energy of the laser pulse. Based on model calculations of the Raman frequencies of the polymer these peaks were attributed to carbon-deuterium and nitrogen-deuterium vibrations and their appearance indicates the occurrence of nuclear reactions in the laser field amplified by plasmonic nanoparticles, involving the polymer atoms.

Keywords: plasmonic enhancement, femtosecond laser, nuclear reactions, Raman spectroscopy, dimethacrylate polymer

1. Introduction

The use of high energy short laser pulses is gaining significance in numerous applications. Localized surface plasmon polaritons (LSP) can for example be excited efficiently with these pulses even up to very high laser intensities. One of the reasons to do so is that with the help of

plasmonic nanoparticles the electromagnetic field of the lasers can be focused to the nanoscale resulting in electromagnetic fields orders of magnitude higher, than that of the laser pulse. Our motivation to explore this amplification effect has been to use these high fields to realize tabletop plasmonic nano-fusion processes [1]. Ti:Sa femtosecond laser pulses have been used to excite LSPs in a polymer sheet, containing resonant plasmonic gold nanorods, with laser intensities up to a few times 10^{17} W/cm². The first step in our studies has been the analysis of the craters formed by individual laser shots in the material [2]. It has been found, that the volume of these craters is always significantly higher in the polymer containing the gold nanoparticles than in the same polymer without them. The volume increase can be attributed only to nuclear processes, and it has been found, that the crater volumes depend linearly on the energy of the laser pulses [2]. Since this energy production has been found to be comparable, or even larger, than that of the energy of the laser pulse, it has been decided to use vibrational spectroscopic method (Raman spectroscopy) to characterize structural changes occurred in the polymeric structure forming the crater walls created upon irradiation with single-shot high-energy femtosecond laser pulse. The irradiation with different pulse energies has been performed on pure polymer and that doped with plasmonic gold nanorods (in two different concentrations) having plasmon resonance at the wavelength of the femtosecond laser, and the Raman measurements were performed on both types of samples.

Raman spectroscopy is widely used to characterize the bonding configuration of different polymeric materials, including dimethacrylates. This method can be used to determine the degree of conversion in these types of polymers, as well, through the changes and ratio of the Raman peak of the C=C double bonds to that of a reference band belonging to a bond not affected by the polymerization [3-5]. In addition to the bonds of the polymer frame it allows to study the different C-H and N-H groups as well.

2. Methods

2.1. Materials and sample preparation

The photopolymerizable dimethacrylate resin mixture consists of urethane dimethacrylate (UDMA) (Sigma Aldrich Co., St. Louis, MO, USA) and triethylene glycol dimethacrylate (TEGDMA) (Sigma Aldrich Co., St. Louis, MO, USA). The weight ratio of UDMA : TEGDMA was 3 : 1. Dodecanethiol-capped gold nanorods (Au-DDT) in size of 25 nm diameter and 75 nm length were purchased from Nanopartz Inc., USA (No. B12-25-700-1DDT-TOL-50-0.25, No. B12-25-750-1DDT-TOL-50-0.25).

The preparation method of undoped (UDMA-X) and doped with gold nanorods (UDMA-Au) polymer samples is described in detail elsewhere [6]. In short, the mixture of the UDMA

and TEGMA monomers and the photoinitiator (and the gold nanorods) was placed on a glass slide in a thin template allowing to obtain a thin layer of the resin. Then the polymerization mixture was irradiated with a standard dental curing lamp emitting blue light with a constant 3 min exposure time. The obtained samples of disc shape were clear (non-doped polymer) or had pink color (Au doped samples). The gold nanorods were added to the monomer mixture in 2 different concentrations of 0.124 m/m% and 0.182 m/m%, and the corresponding samples are marked as UDMA-Au1 and UDMA-Au2 in this manuscript, respectively.

2.2. Laser irradiation experiments

Femtosecond laser illumination was implemented by a Ti:Sapphire-based chirped-pulse two-stage amplifier-laser system (Coherent Hydra) delivering pulses with 40 fs pulse length at 795 nm central wavelength with 10 Hz repetition rate and 25 mJ maximum pulse energy. The sample treatment was achieved by single pulses of different energy that were illuminating different positions of the sample surface. The beam was focused by a lens with 50 cm focal length, and the sample was shifted laterally after each illumination. The laser irradiation experiments were performed under vacuum conditions for avoiding nonlinear processes in air as for example filamenting. The pressure in the vacuum chamber was in the range of 10^{-6} mbar. Since the energy density is above the ablation threshold of the material, crater formation was observed at the focal spot.

2.3. Raman spectroscopic measurements

A Renishaw InVia micro-Raman spectrometer connected to a LeicaDM2700 microscope was used for the Raman spectroscopic measurements. The Raman spectra were recorded on the wall of the formed crater with 532 nm excitation in backscattering geometry, with the laser focused into a spot of ~ 1.3 microns diameter on the sample surface by using an 50X/0.5 NA objective. The laser power was ~ 6 mW that equals to 5-10% of the maximum intensity of the laser source. The spectra were recorded in the $1000 - 2600 \text{ cm}^{-1}$ spectral region. Due to the low intensity of the investigated Raman bands the accumulation time was set to 2 hours in each spot. Before the measurements, calibration was done by using a silicon wafer and its characteristic peak at 520 cm^{-1} Raman shift.

Since this study is about the evaluation and comparison of small intensity Raman peaks recorded on different craters formed upon single-shot laser irradiation, a special care was given to the processing of the measured Raman spectra. The experimental data were processed with the Origin 2019 software and a custom Matlab code. The first step was a background subtraction by

using the Asymmetric Least Squares method [7]. Then, the integral intensity of the peaks of interest were determined by determining the area under the curve for the Raman bands observed in the 2000-2500 cm^{-1} region. In addition, the integral intensity of the C-C peak at 1460 cm^{-1} was also determined. This Raman band used for the normalization of the Raman intensities of the other peaks in the 2000-2500 cm^{-1} region.

2.4. Modeling and calculations of selectively deuterized UDMA monomer

The chemical structure of urethane-dimethacrylate (UDMA) monomer is shown in Figure 1. Part of this structure containing N-H bond and CH_2 groups was selected as a starting geometry for further modeling and subsequent calculations. For better description of the chemical environment, the dangling chemical bonds at the ends of model were terminated with methyl (CH_3) and hydroxyl (OH) groups, as shown in Figure 2.

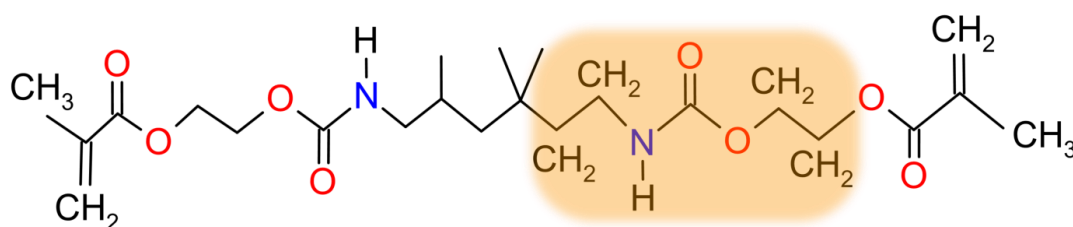


Figure 1. Chemical structure of UDMA monomer together with the selected part used for further modeling and calculations.

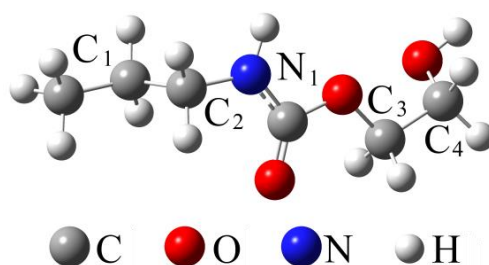


Figure 2. Optimized (B3LYP/6-311++G(d,p)) geometry of UDMA model ($\text{C}_1\text{H}_2\text{-C}_2\text{H}_2$ and $\text{C}_3\text{H}_2\text{-C}_4\text{H}_2$ groups are in anti and gauche conformational states, respectively).

The self-consistent density functional theory (DFT) field method using the hybrid B3LYP functional consisting of a linear combination of the pure corrected exchange functional by Becke [8] and the three-parameter gradient-corrected correlation functional by Lee *et al.* [9] was applied for geometry optimization of UDMA model and Raman spectra calculations using the Gaussian-09 program package [10]. The triple zeta valence (TZV) Pople 6-311++G(d,p) basis set was used for all atoms [11]. The total energy of the gas-phase model was optimized using the Berny optimization algorithm. The vibrational frequencies of model calculated using the same

method and basis set verified the optimized geometry as true energy minimum structure. The Raman activities of the vibrational modes of UDMA model were also calculated. To study the effect of selective deuterization on the Raman spectra of UDMA model, the C₁H₂, C₂H₂, C₃H₂, C₄H₂ and N₁H groups (hereafter denoted as C₁, C₂, C₃, C₄ and N₁ sites) were used for hydrogen-to-deuterium substitution (Figure 2). The optimized structure of UDMA models were used for further vibrational mode frequency calculations of selectively deuterated structures. For this reason the exact mass of the deuterium isotope (2.01410 a.m.u.) was used for hydrogen atoms bonded to the selected site (centre).

To simulate the Raman spectra of the model a Lorentz-shape function with the intensity proportional to the calculated Raman activity and with full width at half-height (FWHH) of 20 cm⁻¹, modeling the natural band width of the experimental spectra, was applied for each of the computed Raman modes.

3. Results and discussion

3.1. Differences in the Raman spectrum of the crater wall in samples with and without gold nanorods

Figure 3 shows the Raman spectra recorded on several different craters formed upon single-shot irradiation of the UDMA polymer with and without gold nanorods with laser pulses of different energy in the 1950-2600 cm⁻¹ spectral region. While both groups of spectra show a relatively strong photoluminescence background, some well-resolved bands can also be observed in the spectra of the UDMA-Au samples. The two broad peaks have maxima around 2100 cm⁻¹ and 2400 cm⁻¹ and their intensity seems to be dependent on the laser pulse energy. These features are difficult to observe in the spectra of the non-doped samples (however a weak and broad band between 2050 and 2500 cm⁻¹ can be resolved there as well).

Since the two UDMA samples used for the irradiation experiments were fabricated from the same monomer mixture, and the only difference is the addition of the gold nanorods to the monomer mixture, it can be assumed that the two Raman peaks appearing in the spectra of the UDMA-Au sample upon irradiation are related to the presence of the gold nanoparticles.

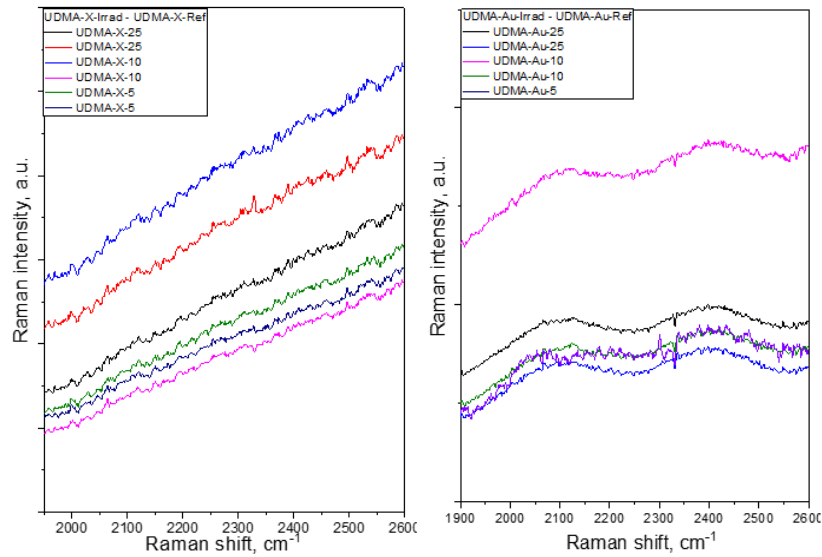


Figure 3. Raman spectra of the craters formed upon single-shot pulsed laser irradiation of UDMA samples with (UDMA-Au) and without (UDMA-X) gold nanorods with pulses of different energy.

The dependence of the integrated intensity of the two Raman bands on the laser pulse energy for the UDMA samples without and with gold nanorods of two different concentrations is shown in Fig. 4. The Figure contains values for two Raman measurements in each crater. It can be seen that for the UDMA-X sample the peak intensity is 0.067 and does not change with the pulse energy. Some variation can be observed for the UDMA-Au1 sample, where the band intensity slightly decreases up to 5 mJ (to 0.083, yet above the value for the UDMA-X sample), but then increases to 0.204 (0.123 for the second shot) at 25 mJ pulse energy. The increase of the peak

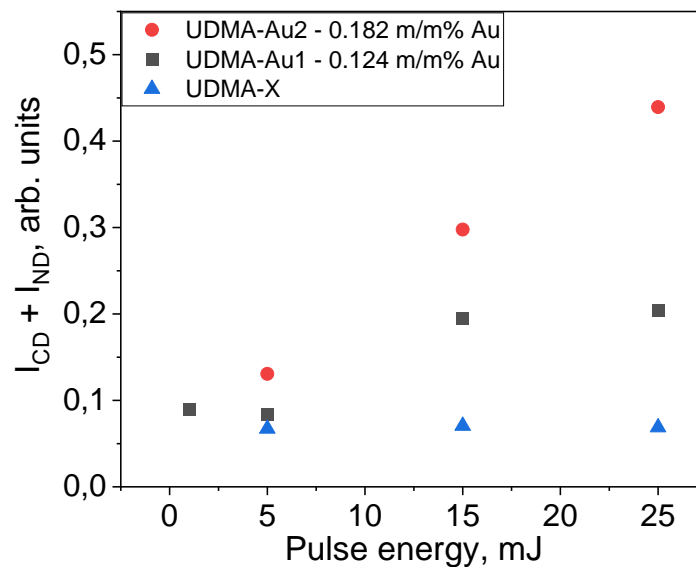


Figure 4. Dependence of the integrated intensity of the Raman bands in the 2000-2500 cm^{-1} region of the Raman spectra recorded on the crater walls on the laser pulse energy.

area is even more pronounced for the UDMA-Au2 sample, where it starts from 0.131 for 5 mJ and reaches 0.459 (0.256 for the second shot) at 25 mJ. The observed behavior also supports that the new peaks appearing in the 2000-2500 cm^{-1} region are related to the presence of the gold nanorods.

Another series of Raman measurements were performed on 5 different craters formed upon irradiation of a new set of UDMA-X, UDMA-Au1 and UDMA-Au2 samples with 25 mJ pulse energy. The integrated peak intensities for the 2000-2500 cm^{-1} region are compared in Figure 5. It can be seen that the UDMA-X sample has lowest band intensities that show minimal fluctuation in the different craters. Both UDMA-Au1 and UDMA-Au2 show higher peak intensities that have large crater-to-crater variance. These findings are in good agreement with the earlier observations (Fig. 4).

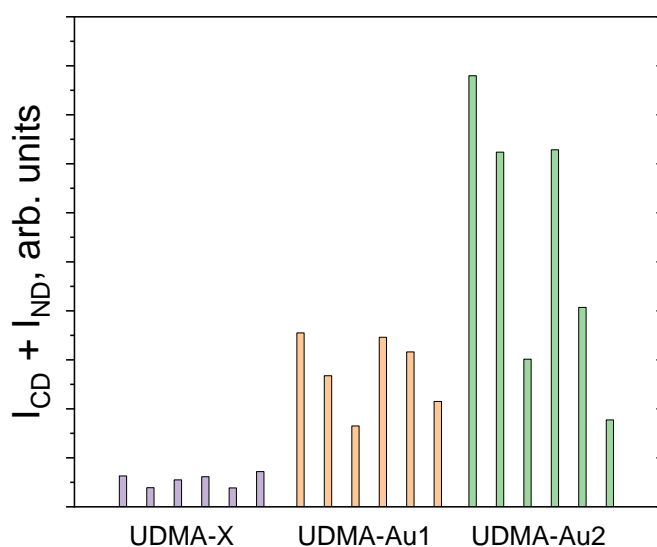


Figure 5. Integrated intensity of the Raman bands in the 2000-2500 cm^{-1} region of the Raman spectra recorded on separate craters formed upon irradiation of the samples with 25 mJ laser pulse energy.

The relation between the Raman bands in the 2000-2500 cm^{-1} region is also supported by the variance in the peak intensity. Since the polymer contains the gold nanoparticles in a relatively small density, the Raman spectra are recorded in areas incorporating gold nanoparticles in different amounts. As a consequence, the band intensities will fluctuate in a broad range. On the other hand, the UDMA-X sample is completely homogeneous, it can be expected that the Raman peak intensity will be the same, independently on the place of the measurement – and this can be observed in both Figs. 4 and 5.

The appearance of the new Raman peaks is related to the presence of gold nanoparticles. Since gold has no stable bonds with carbon, nitrogen, oxygen and hydrogen, the chemical origin,

namely the formation of some new structural units involving gold can be excluded. The plasmonic effect of the nanorods, however, is of high probability. Since the plasmon resonance of the nanoparticles along their long axis is tuned to the wavelength of the femtosecond pulsed laser used for the single-shot treatment, these nanostructures act as nanoantennas and amplify the electromagnetic field of the incident light in their surrounding. This enhancement could reach a few orders of magnitude and presumably this field, being much stronger than that in the non-doped UDMA, is responsible for the difference in structural transformations and the appearance of the new Raman features in the 2000-2500 cm^{-1} region.

The new bands appearing in the 2000-2500 cm^{-1} region of the Raman spectrum of the craters formed upon irradiation of UDMA samples doped with gold nanorods could have three possible origins. They could arise from some contamination, be not a Raman but a photoluminescence feature or belong to some new structural units. The contamination can be excluded, since the UDMA-X, UDMA-Au1 and UDMA-Au2 samples were prepared from the same monomer mixture in each of the two sample sets, but the peaks are not present in the UDMA-X sample. In addition, the gold nanorods were of high purity and two different batches were used for the two sample sets.

The width of the two peaks is 100-150 cm^{-1} that corresponds to 3.7-5.5 nm on the wavelength scale. Photoluminescence peaks of this small width are characteristic for molecules and not for bulk polymeric samples, so this origin can be excluded as well.

The third possible assignment of the new peaks is the formation of new structural units. The host UDMA polymer contains different C-H, N-H, C=C, C-O and C=O bonds and corresponding functional groups. none of these could have Raman peak in the 2000-2500 cm^{-1} region. With the elements present in UDMA alkyne (C \equiv C), nitrile (C \equiv N), azide (N=N=N), and carbon-deuterium (C-D) bonds were found to have Raman bands in the 2000-2300 cm^{-1} region [12]. The alkyne bond is the least stable from the possible C-C bonds, therefore its formation upon laser irradiation is of small probability. The same is true for the azide group, since the UDMA monomer contains only two nitrogen atoms per monomer, so the conditions are not favorable for the formation of triple nitrogen chains. Formation of nitrile is possible, but this bond has a Raman peak around 2220-2260 cm^{-1} , which is right in-between the band positions observed in the Raman spectra (see Fig. 3). The different C-D bonds, however, have their Raman peak in the 2000-2200 cm^{-1} region, which is in good agreement with the position of one of the peaks observed in the Raman spectrum. This assignment suggests that deuterium atoms were formed during the interaction of the ultrashort laser pulse with the polymeric structure, when the local electromagnetic field was enhanced by the plasmonic gold nanorod antennas. These deuterium

atoms are formed from hydrogen atoms being attached to the polymer during the reaction or are free atoms that substitute these hydrogens. As a consequence, carbon-deuterium groups form, and the corresponding peak can be detected in the Raman spectrum in the 2000-2200 cm^{-1} region.

Assuming this origin, the deuterons will be attached not only to the carbon atoms in the UDMA frame, but also to nitrogen. A simple estimation of the shift of the N-H Raman peak position at 3465 cm^{-1} upon the N-H to N-D substitution gives the latter to be around 2500 cm^{-1} , which is in good correlation with the position of the second peak observed in the Raman spectrum (see Fig. 2).

In order to verify this hypothesis, density functional theory calculations were performed to determine the Raman peak positions of the different C-D and N-D structural units.

3.2. DFT calculations of UDMA monomer during H-to-D substitution

Figure 6 shows the spectral region characteristic of C-H and N-H stretching vibrations in the simulated Raman spectra of the four UDMA models (see Fig. 1). The C-H vibrations are in the 2800-3000 cm^{-1} region, while the N-H band is around 3465 cm^{-1} . The tentative band assignments are given in Table 1. It can be seen that the bands in the 2800-3000 cm^{-1} region are related to symmetric and asymmetric vibrations of the CH_2 group being in different bonding configurations. The NH group has only one vibrational frequency.

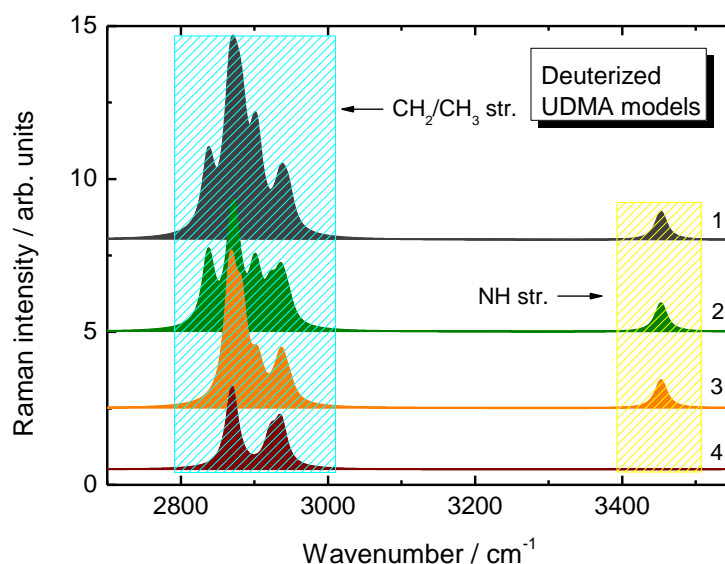


Figure 6. Spectral region of CH and NH stretching vibrations in the simulated Raman spectra of natural UDMA model (Fig. 2). The simulated spectra were frequency corrected by using the scaling factor of 0.95.

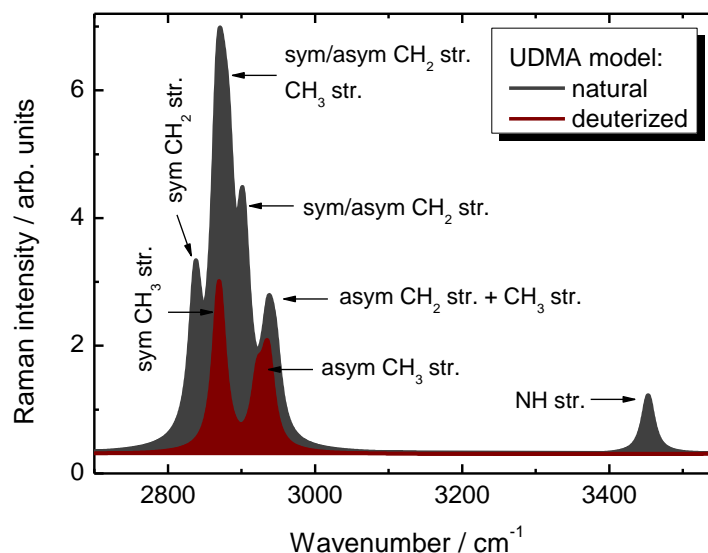


Figure 7. Assignment of the Raman peaks obtained in the simulated Raman spectra of natural UDMA model. The simulated spectra were frequency corrected by using the scaling factor of 0.95.

Table 1. Calculated (6-311++G(d,p)) vibrational frequencies (ν , cm^{-1}) and Raman activities (RA, $\text{\AA}^4/\text{a.m.u.}$) of natural (H) and deuterized (D) UDMA models together with mode assignments. All the calculated mode frequencies were corrected by using scaling factor 0.95.

ν_D	RA_D	ν_H	RA_H	Assignment
2062	69.4	2837	147.1	sym C(H/D) ₂ str. (OH)
2088	59.6	2867	165.9	sym C(H/D) ₂ str. (CH ₃)
2101	48.6	2882	169.2	sym C(H/D) ₂ str. (NH)
2108	74.3	2901	118.0	sym C(H/D) ₂ str. (OC)
2136	45.6	2875	96.7	asym C(H/D) ₂ str. (OH)
2155	42.1	2904	75.4	asym C(H/D) ₂ str. (CH ₃)
2184	10.3	2946	31.1	asym C(H/D) ₂ str. (NH)
2188	21.2	2945	35.1	asym C(H/D) ₂ str. (OC)
2530	34.0	3453	68.4	N(H/D) str.

sym str. and asym str. - symmetric and asymmetric stretching vibrations, respectively.

Figure 8 shows the simulated Raman spectra of UDMA models selectively deuterated at C₁-C₂, C₃-C₄ and N₁ sites (see Fig. 2) in the region of C-D and N-D stretching vibrations. As can be seen, the selective H-to-D substitution at C sites of UDMA models lead to appearance of bands in the region of 2000-2200 cm^{-1} , characteristics of CD₂ stretching vibrations. In addition to the location of particular CD₂ group (*i.e.* nearest neighbour atoms), the frequency position of these bands are found to be dependent on conformational state (gauche and anti) of CD₂ groups (Figure 8, curve 1 and 2). The Raman band at 2530 cm^{-1} characteristics of N-D stretching vibrations was calculated for UDMA model deuterized at N₁ site (Figure 8, curve 3). The superposition of C-D stretching vibrations of different CD₂ groups form the broad band in the

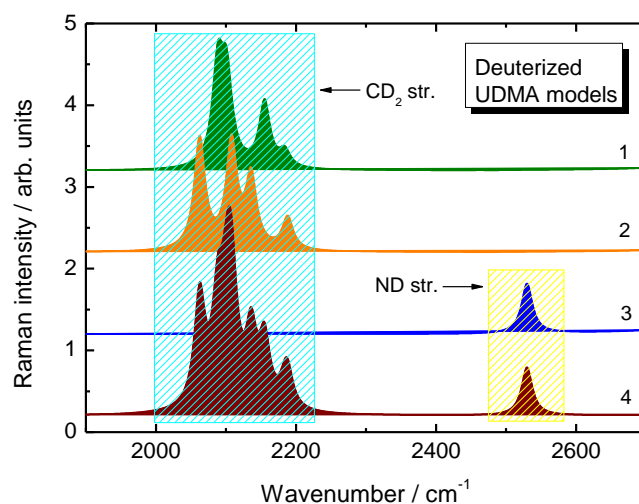


Figure 8. Spectral region of CD and ND stretching vibrations in the simulated Raman spectra of UDMA model used for selective H-to-D substitution at C_1D_2 - C_2D_2 (1), C_3D_2 - C_4D_2 (2) and N_1D (3) groups together with the fully (all groups) deuterized state (4). The simulated spectra were frequency corrected by using the scaling factor of 0.95.

2000-2200 cm^{-1} region of simulated Raman spectra of fully (C_1 - C_2 , C_3 - C_4 and N_1 sites) deuterized UDMA model are shown in curve 4 of Figure 8. The assignment of the Raman bands is given in Table 1. It should be noted that in case of the natural model some of the CH modes are coupled, and for them the frequency change is not monotonic/proportional during H-to-D substitution.

Conclusions

Raman spectroscopic measurements were performed on the crater walls formed in urethane dimethacrylate - triethylene glycol dimethacrylate polymer containing plasmonic gold nanorods upon irradiation with a single-shot high energy femtosecond laser pulses of different energy. New Raman bands were detected in the 2000-2500 cm^{-1} region of the Raman spectrum the intensity of which shows strong dependence on the presence/concentration of the plasmonic nanoparticles and the energy of the laser pulse. Based on model calculations of the Raman frequencies of the polymer these peaks were attributed to carbon-deuterium and nitrogen-deuterium vibrations and their appearance indicates the occurrence of nuclear processes involving the polymer in the laser field amplified by plasmonic nanoparticles, forming hotspots at their surface. These results at these relatively low laser pulse energies (intensities) are encouraging for our plans to continue our studies at much higher energies to reach economically feasible tabletop nuclear fusion.

Acknowledgments

This work was supported by Nanoplasmonic Laser Fusion Research Laboratory project financed by the National Research and Innovation Office (NKFIH-468-3/2021) and by the Eötvös Lóránd Research Network (ELKH), Hungary. The research reported in this paper and carried out at the Budapest University of Technology and Economics has been supported by the NRDI Fund (TKP2020 IES, Grant No. BME-IE-BIO) based on the charter of bolster issued by the NRDI Office under the auspices of the Ministry for Innovation and Technology. This work was supported by the VEKOP-2.3.2-16-2016-00011 grant, which is co-financed by the European Union and European Social Fund.

References

1. L.P. Csernai, M. Csete, I.N. Mishustin, A. Motornenko, I. Papp, L.M. Satarov, H. Stöcker & N. Kroó, Radiation-Dominated Implosion with Flat Target, *Physics and Wave Phenomena*, 28 (3) 187-199 (2020). (arXiv:1903.10896v3).
2. Á. Nagyné Szokol et al. Crater formation upon single-shot femtosecond laser irradiation in dimethacrylate polymer doped with plasmonic gold nanorods (in preparation)
3. Mahmood, M.H.; Himics, L. ; Váczi, T. ; Rigó, I. ; Holomb, R. ; Beiler, B. ; Veres, M., Raman spectroscopic study of gamma radiation-initiated polymerization of diethylene glycol dimethacrylate in different solvents; *JOURNAL OF RAMAN SPECTROSCOPY* 52 : 10 pp. 1735-1743. , 9 p. (2021)
4. Par, M.; Gamulin, O.; Marovic, D.; Klaric, E.; Tarle, Z. Raman spectroscopic assessment of degree of conversion of bulk-fill resin composites—Changes at 24 hours post cure. *Oper. Dent.* 2015, 40, E92–E101
5. BinMahfooz, A.M.; Qutub, O.A.; Marghalani, T.Y.; Ayad, M.F.; Maghrabi, A.A. Degree of conversion of resin cement with varying methacrylate compositions used to cement fiber dowels: A Raman spectroscopy study. *J. Prosthet. Dent.* 2018, 119, 1014–1020
6. Bonyár A et al. The effect of femtosecond laser irradiation and plasmon field on the degree of conversion of a UDMA-TEGDMA copolymer nanocomposite doped with gold nanorods, *Nanomaterials* (2022)
7. Eilers, Paul & Boelens, Hans. (2005). Baseline Correction with Asymmetric Least Squares Smoothing. Unpubl. Manuscr.
8. A.D Becke, Density-functional exchange-energy approximation with correct asymptotic

- behavior, Phys. Rev. A. 38 (1998) 3098-3100. <https://doi.org/10.1103/PhysRevA.38.3098>
9. C. Lee, W. Yang, R.G. Parr, Development of the Colle-Salvetti correlation-energy formula into a functional of the electron density, Phys. Rev. B., 37 (1998) 785-789. <https://doi.org/10.1103/PhysRevB.37.785>
 10. M.J. Frisch, G.W. Trucks, H.B. Schlegel, G.E. Scuseria, M.A. Robb, J.R. Cheeseman, G. Scalmani, V. Barone, B. Mennucci, G.A. Petersson, H. Nakatsuji, M. Caricato, X. Li, H.P. Hratchian, A.F. Izmaylov, J. Bloino, G. Zheng, J.L. Sonnenberg, M. Hada, M. Ehara, K. Toyota, R. Fukuda, J. Hasegawa, M. Ishida, T. Nakajima, Y. Honda, O. Kitao, H. Nakai, T. Vreven, J.A. Montgomery Jr., J.E. Peralta, F. Ogliaro, M. Bearpark, J.J. Heyd, E. Brothers, K.N. Kudin, V.N. Staroverov, R. Kobayashi, J. Normand, K. Raghavachari, A. Rendell, J.C. Burant, S.S. Iyengar, J. Tomasi, M. Cossi, N. Rega, J.M. Millam, M. Klene, J.E. Knox, J.B. Cross, V. Bakken, C. Adamo, J. Jaramillo, R. Gomperts, R.E. Stratmann, O. Yazyev, A.J. Austin, R. Cammi, C. Pomelli, J.W. Ochterski, R.L. Martin, K. Morokuma, V.G. Zakrzewski, G.A. Voth, P. Salvador, J.J. Dannenberg, S. Dapprich, A.D. Daniels, O. Farkas, J.B. Foresman, J.V. Ortiz, J. Cioslowski, D. J. Fox, Gaussian 09, Revision A.02, Gaussian, Inc., Wallingford CT, 2009.
 11. V.A. Rassolov, J.A. Pople, M.A. Ratner, T.L Windus, 6-31G* basis set for atoms K through Zn, J. Chem. Phys. 109 (1998) 1223-1229. <https://doi.org/10.1063/1.476673>
 12. H. Yamakoshi, J. Am. Chem. Soc., 2012